Journal of Physics: Conference Series **457** (2013) 012009 doi:10.1088/1742-6596/457/1/012009

Emergence of the coherent reflected field for a single realisation of spherical scatterer locations in a solid matrix

V J Pinfield and R E Challis

Electrical Systems and Optics Division, Faculty of Engineering, University of Nottingham, University Park, Nottingham NG7 2RD, UK

Email: valerie.pinfield@nottingham.ac.uk

Abstract. The acoustic field reflected from a region containing spherical scatterers is most often estimated by use of the coherent field; that is, the field resulting from the summed scattered fields from the scatterers, averaged over all possible configurations of scatterer locations. It is this ensemble-averaged coherent field which is equivalent to the field reflected from a homogeneous medium with properties which can be derived mathematically using ensemble-averaging techniques. Such properties include the effective density, and the effective wavenumber, which can be derived from multiple scattering theories, or by other homogenisation methods. Experimentally, although ensemble-averaging can be effected in practice in fluid systems due to the motion of the scatterers during the measurement time-scale, measurements in solid materials have fixed locations of scatterers. Averaging can only be achieved by using "large" sample areas, multiple samples or measurements in different locations, or "large" receiver areas. However, in the context of NDE applications we are interested in the field resulting from a specific region of material, rather than the average over a large region. Our study addresses the question of when the coherent field (resulting from averaging over many scatterer configurations) can be used as an accurate description of the field reflected by a region of scatterers at fixed locations. In this paper we present results of simulations of the scattered reflected field from a region of solid material containing spherical cavities. Simulations of single realisations of scatterer locations are compared with the coherent field, to demonstrate the validity or otherwise of the use of the coherent field to describe the response of a particular configuration of scatterers.

1. Introduction

The field of acoustic wave propagation in heterogeneous materials has a long history and remains a topic of study due to its range of significant applications. One such application is the use of ultrasonic non-destructive testing techniques for aerospace components, which has prompted the current work. Our interest is in the signal backscattered from a region of small cavities in a composite material.

The majority of published work concerned with acoustic propagation in heterogeneous media considers the coherent field, that is the field which has the same characteristics as that propagating in a homogeneous medium, but with modified properties. This coherent field emerges only on averaging the locations of scatterers, a process known as ensemble-averaging, or homogenization [1]-[5]. The properties of the equivalent homogeneous medium or effective medium resulting from the coherence condition can be used to define the response of the material. These properties include the effective wavenumber, which is widely used to obtain the speed of wave propagation in materials. In an experimental measurement, the ensemble averaging process may be effected by measurements over a

large area of sample, multiple samples, a large received area, or by a time-averaging (if scatterers are mobile). In some circumstances however, we are interested in the response of a particular region of material, which may not be coherent, since the scatterers are fixed and the region small.

In this study, we investigate the conditions for coherence for a particular configuration, in which the response of a plane slab of scatterers in a solid matrix is simulated, using a single receiving point. Thus we eliminate the effects of averaging at the receiver, but consider the response of a planar region. A range of simulations has been carried out to investigate the emergence of the coherent field over a range of cavity radii and concentrations (number density). We establish the dependence of the degree of incoherence of the field with these parameters compared with the wavelength. We also investigate the variability in the degree of incoherence of the signal.

2. The models

The computational models for the study of the backscattered field have been presented in previous papers [6]-[7] and only a brief summary is presented here.

2.1. Discrete scatterer model

Scatterers are located randomly within a solid matrix, in a slab region as shown in Figure 1a. A transmitting and receiving surface is coupled directly to the solid and its response is assumed to relate to the normal displacement at the surface. The incident field at each scatterer is assumed to be the plane wave transmitted from the surface. The discrete scatterer model simulates the field at a point on the receiving surface obtained from the sum over the scattered fields from each scatterer. The scatterers are taken to be spherical cavities of identical radius. Only single scattering is considered, and the anisotropy of the scattered field is included using the far-field scattering amplitude, derived from Rayleigh partial wave expansions according to the method of Ying and Truell [8].

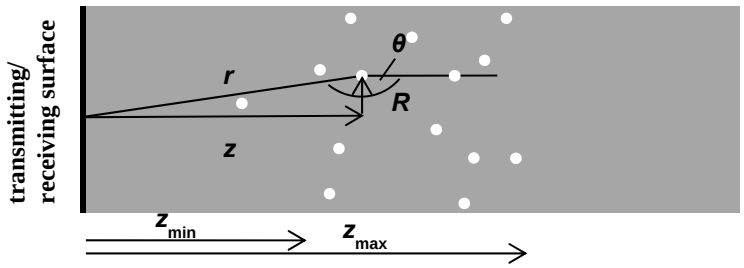

(a)

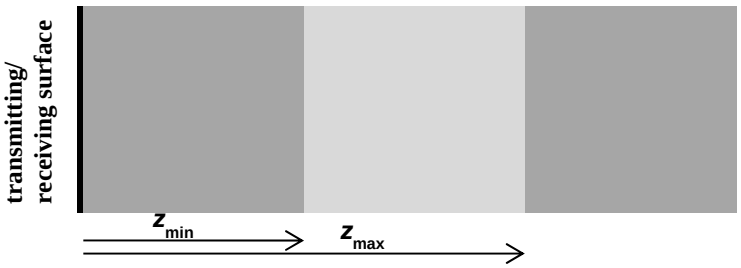

(b)

Figure 1 Configuration of the models: (a) discrete scatterer model (above dashed line) and (b) effective medium model (below dashed line). The coordinates (z,R) of a cavity relative to the receiving point are shown.

The normal displacement at the receiving surface is given by

$$\mathbf{u}_{z,\mathrm{mult}} = \mathbf{u}_{z,\mathrm{inc}} \sum_{j=1}^{N_{sc}} e^{ikz_j} \cdot \frac{e^{ikr_j}}{r_j^2} \left[-\left.\frac{\partial f(\theta)}{\partial \theta}\right|_{\theta_j} \sin\theta_j - ikz_j \cdot f(\theta_j) \left\{ 1 - \frac{1}{ikr_j} \right\} \right] \tag{1}$$

where the far-field amplitude is related to the scattering coefficients by

$$f(\theta) = \frac{1}{ik} \sum_{n=0}^{\infty} (2n+1) A_n P_n(\cos\theta) \tag{2}$$

The wavenumber in the solid matrix is denoted by k and the angle, θ, is taken relative to the forward z-direction. P_n are the Legendre polynomials and r is the distance from the scatterer to the receiving point. The normal displacement of the transmitted plane wave at the transmitting surface is $\mathbf{u}_{z,\mathrm{inc}}$. The notation for the scattering coefficients, A_n, is adopted from earlier references, and is presented in [9].

In the discrete scatterer model, there are no interfaces between the solid matrix and the region containing scatterers. The model predicts the response from a single realisation of scatterer locations for a particular cavity radius and number density (expressed as a volume fraction).

2.2. Ensemble-average model

An estimate of the ensemble-average limit, that is the coherent field, is obtained by numerical integration over the discrete scatterer model field equations using random locations for scatterers.

2.3. Effective medium model

In the effective medium model, the region containing scatterers is replaced by a homogeneous material (Figure 1b) whose properties are assigned using ensemble-averaged scattering theory formulations. Thus in this model, there are interfaces at the front and back of the slab region at which the material properties change. The effective density used in the model is the volume averaged density.

$$\rho_{\mathrm{eff}} = \rho(1-\phi) \tag{3}$$

where ϕ is the volume fraction of cavities and ρ is the density of the solid matrix. The Foldy wavenumber [1] was used to obtain the wave speed, taking the same partial Rayleigh wave analysis for the scattering coefficients [9].

$$\left(\frac{K_{\mathrm{eff}}^2}{k^2} \right) = 1 + \frac{3\phi}{k^2 a^3} f(0) \tag{4}$$

where a is the radius of the cavities and K_{eff} is the effective wavenumber of the region. These properties are used to define an effective impedance for the layer, permitting standard reflection and transmission coefficients to be assigned to the interfaces. Thus the reflected coherent signal can be expressed in the usual way as

$$\mathbf{u}_{z,\mathrm{eff}}(\omega) = \mathbf{u}_{z,\mathrm{inc}}\, e^{2ikz_{\min}} \cdot r_{12} \left[1 - t_{12}t_{21}\, e^{2ikd} \left\{ 1 - r_{12}^2\, e^{2ikd} \right\}^{-1} \right] \tag{5}$$

where $d = z_{\max} - z_{\min}$ is the thickness of the layer and r_{ij}, t_{ij} are the displacement reflection and transmission coefficients between regions i and j. Region 1 is between the transmitter and the slab, and region 2 is the slab region whose effective properties are under consideration.

These models incorporate some simplifications in order to enable the simulation of a large slab region. Other workers have studied the coherent field using techniques such as finite difference methods, which are constrained to smaller scale simulations, but are able to adopt higher order assumptions on the incident field for example. Since we are interested in the emergence of the coherent field and its dependence on the length scales of the system, we consider the field at a single point on the receiving surface in order to remove any effects of averaging at the receiver.

2.4. Numerical calculations

Numerical calculations were carried out using Matlab. The fields were calculated in the frequency domain with a sampling frequency of 50 MHz and 1024 samples. Time-domain results were obtained using experimentally sampled transmit-receive signals to model the transmitted signal for a 5,10 MHz centre-frequency transducer. A range of cavity radii from 5-20 μm and concentrations by volume of 1-20% were simulated. Each discrete scatterer model simulation represents a single realization of cavity locations, all of the same size. The solid matrix was assigned properties appropriate to an averaged fibre-resin composite, with a longitudinal wave speed of 3035 ms^{-1}, a density of 1564 kgm^{-3}, and a shear modulus of 3.6 GPa. The simulation aims to represent the response of a slab, but must be constrained in the lateral direction for calculation purposes. Tests showed that a maximum radial coordinate of R_{max}=20 mm (see Figure 1) was sufficient to capture the full response. Other system parameters are listed in Table 1.

Table 1. System parameters.

Distance z_{min} /mm	2
Layer thickness / mm	1
Cavity conc / v/v%	1, 2, 5,10, 20
Cavity radius / μm	5.0, 7.9, 10.0, 15.9, 20.0
Millions of cavities at 20 v/v% (respectively with radius)	480, 120, 60, 15, 7.5

All time-domain results have been plotted time-shifted to the arrival of the first reflection from the front of the layer and have been scaled by concentration for ease of comparison. Frequency-domain results were windowed in the time domain to smooth out the edge-wave ripples caused by truncation of the region. Fuller details of the simulation are given in [6]-[7].

3. Results

3.1. Time-domain results

Results of the models are shown in Figure 2 in the time-domain using signals with centre frequencies (c.f.) of 5 and10 MHz. The results have been scaled by concentration for convenience of comparison. In each figure, the coherent response (from the effective medium model) can be seen to display reflections from the front and back of the layer with the appropriate time delay between them. However, the discrete scatterer responses (in black) show varying degrees of agreement with this coherent field. In Figure 2a, the discrete scatterer response for 10 μm radius cavities at 2%, with a 10 MHz c.f. signal, shows a relatively high degree of incoherence, although the initial response is similar to the front face reflection in the coherent field. There is a significant signal between the two coherent reflections, and after them, and the back-wall reflection in the coherent response is not clearly identifiable. At a higher concentration Figure 2b, some of the incoherence is reduced, especially the signal received after the termination of the coherent field. Reducing the radius has a more marked effect at improving coherence. Comparison of Figure 2b (for 10 μm radius) and Figure 2c (for 5 μm radius) shows that the reduction in radius produces a nearly-coherent field at 10% concentration (by volume) with a 10 MHz c.f. signal. It should be noted that since these are at the

same *volume* concentration, the number density is significantly larger at the smaller radius. There is, however, a difference in arrival time of the back wall echo between the discrete scatterer and effective medium models, because the discrete scatterer model is a single scattering model, and is not able to predict the change in effective wave speed due to the porosity, which does occur in the coherent field. A reduction in the centre frequency of the signal also has a significant effect in the emergence of the coherent response from the discrete scatterer model, as seen by comparing Figure 2b (a 10 MHz c.f. signal) and Figure 2d, which shows the response with a 5 MHz c.f. In this case, both front and back-face reflections of the coherent field are produced from this single realization of scatterers in the discrete scatterer model. The difference in arrival time is also clear here, but the plane-wave-like behavior arising from the discrete scatterer model for these single realisations is apparent. Comparisons between various pairs of these figures indicate that coherent field emerges at lower frequency, smaller cavity radius (at constant volume concentration) and higher concentrations.

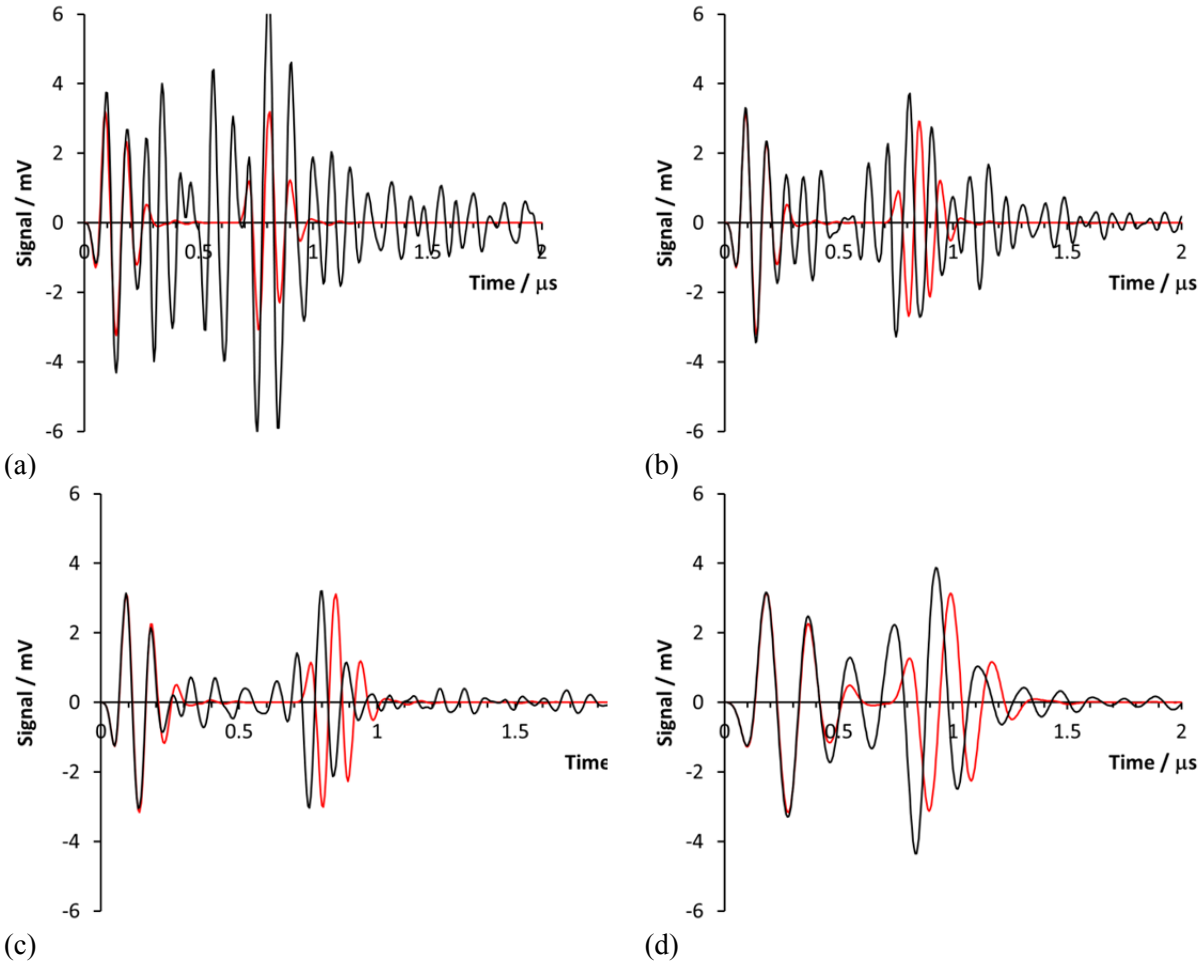

Figure 2 Time-domain results of discrete scatterer (black) and effective medium model (red) simulations for various cavity radii, concentrations and signal centre frequencies (c.f.) (a) 10 µm radius, 2 v/v% with 10 MHz c.f. (b) 10 µm radius, 10 v/v% with 10 MHz c.f. (c) 5 µm radius, 10 v/v% with 10 MHz c.f (d) 10 µm radius, 10 v/v% with 5 MHz c.f.

3.2. Frequency-domain results

In the frequency domain, the response to a time-domain impulse is typical of that of a thick layer for the effective medium model, showing regularly spaced resonance peaks (Figure 3). The integrated

ensemble-average response is also shown (in blue) illustrating a close agreement with the effective medium model, with a slight difference in peak spacing due to the difference in sound speed between the ensemble average (single scattering model) and the effective medium model. Figure 3 also shows the response from the discrete scatterer model (in black) for a single realisation of scatterer locations, for a cavity radius of 10 μm at a concentration of 2% (scaled by concentration). Whilst the discrete scatterer response matches that of the effective medium model at the lowest frequencies, i.e. is a coherent response, it rapidly diverges as the frequency increases, showing increased incoherence.

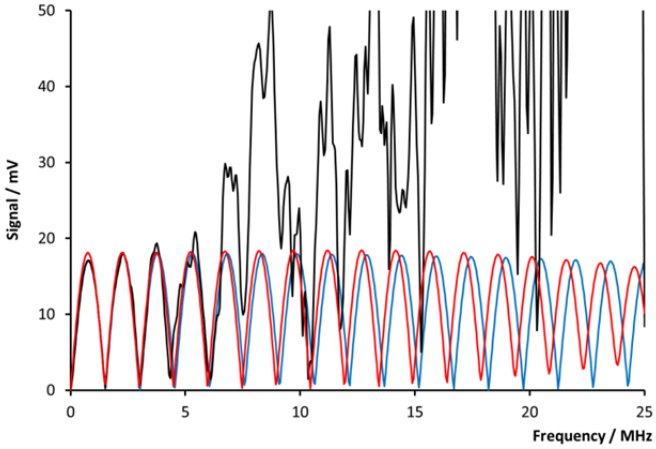

Figure 3 Frequency domain response for a slab of cavities of 10 μm radius for the effective medium model (red) and integrated ensemble average model (blue), and the discrete scatterer model at 2 v/v% (scaled by concentration).

3.3. Deviation from coherence

In order to investigate the conditions for the emergence of the coherent field from the incoherent response of a single realisation of scatterers, we quantify the degree of incoherence using the frequency domain response, such as that shown in Figure 3. As the measure of the degree of incoherence, we have adopted the sum of the squared residuals (RSS) between the discrete scatterer response and a reference response, taken to be either the effective medium (coherent) or ensemble average response. The sum is taken up to each frequency in turn. The RSS is normalised by cumulative sum of the square of the reference response. Further details are provided in [7]. A higher value of RSS indicates a less coherent response. The RSS value increases strongly with frequency (or bandwidth), and is also higher for larger cavity radii (at constant volume concentration), and for lower concentrations; these trends in the degree of coherence were previously observed in the time-domain responses of Figure 2.

The trends in the degree of coherence were established quantitatively by specifying a maximum value of RSS (relative to the effective medium response) which produced a coherent response; this value was estimated by assessing which time-domain responses were acceptably coherent. This maximum value of RSS=0.3 was then used to determine the maximum bandwidth (frequency) permitted to operate within this limit, for each condition of radius and concentration. The criterion is thus equivalent to specifying the maximum frequency at which a coherent response could be expected, for a single realisation of scatterers, for the particular cavity radius and concentration. Figure 4 shows how the maximum frequency varies with cavity radius and concentration for a single realisation at each condition. At larger cavity radius, a lower operating frequency is required to obtain coherence at the same concentration. Conversely, a lower frequency is required when working at lower concentrations of cavities at the same radius.

Power-law fits of the maximum frequency, f_{max} as a function of radius, a, and volume fraction, ϕ (each for a single realisation of the discrete scatterer model) were determined according to the relation

$$f_{\max}/\mathrm{MHz} \approx D\left(a/\mu m\right)^{\alpha} \phi^{\beta} \tag{6}$$

where the fitted values are α=-0.71, β=0.32 with a constant factor D=36.7 (in appropriate mixed units). These fits are shown by coloured lines on Figure 4. It might be expected that the limit for coherent response would be related to the magnitude of the wavelength, compared with the mean distance between scatterers, as a measure of the typical length scale of heterogeneity in the system. This is equivalent to a coherence limit defined by the number density of scatterers per cubic wavelength. This was tested by an alternative power law fit (shown in black on Figure 4) where

$$f_{\max}/\mathrm{MHz} \approx \left(G/\mathrm{ms}^{-1}\right)\left(a/\mu\mathrm{m}\right)^{-1} \phi^{1/3} \tag{7}$$

which resulted in a fit of G=335.1 ms^{-1}, corresponding to around 8 scatterers per (linear) wavelength. This functional dependence, however, does not appear to fit the data so well, as is clear on the plots, especially at small radius and high concentration.

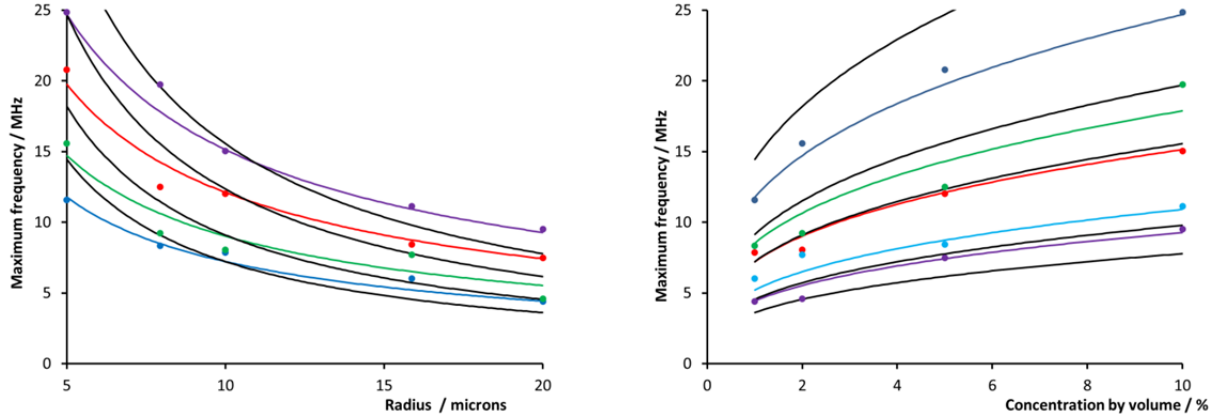

(a) (b)

Figure 4 Maximum bandwidth plotted against (a) radius and (b) concentration of cavities (a) concentrations of [1,2,5,10 %] are represented by blue, green, red, purple symbols respectively (b) radii of [5.0,7.9,10.0,15.9,20.0 μm] represented by blue, green, red, light blue, purple. The coloured fitted lines are given by equation (6), and the black fitted curves are for the fit on number density in equation (7).

3.4. Variability of incoherence

Thus far, the discrete scatterer results shown here have been for only a single realisation of scatterer locations. Since the configuration of scatterer locations is random, a different field response will be obtained for each new realisation, for a fixed cavity radius and concentration. The discrete scatterer model response averaged over many realisations will of course be the coherent field, since it that is an ensemble average response. However, each of the individual discrete scatterer model responses will be incoherent, and deviate from the coherent field by a different degree. By taking many realisations, we obtain the mean degree of incoherence, and the spread of that quantity. This has been determined using 15 simulations of the discrete scatterer model for a cavity radius of 10 μm for each concentration. The sum of squared residuals (RSS) was calculated between each discrete scatterer response (scaled by concentration) and the ensemble average response. Then, the mean and standard deviation of the RSS were calculated. The results are shown in Figure 5 as a function of frequency for the various concentrations; the curves are considerably smoothed compared with the results from any single realisation. Figure 5 shows the mean +/- one standard deviation shown by error bars, demonstrating the high degree of variation in the RSS value for different realisations of the same system. The RSS relative to the effective medium response (true coherent response) are similar, but

include the error due to the effective wave speed which is not accounted for in the discrete scatterer and ensemble average models. Due to the spread of RSS values under the same conditions (radius, frequency, concentration), the definition of a coherent response condition would therefore require a confidence limit specification based on the standard deviation, to ensure that any single realisation would be likely to fall within an acceptable coherence level. At the approximate coherence condition obtained here, the standard deviation in RSS is around half the mean. Thus any definition of the coherence condition must consider the likely range of single realisation responses.

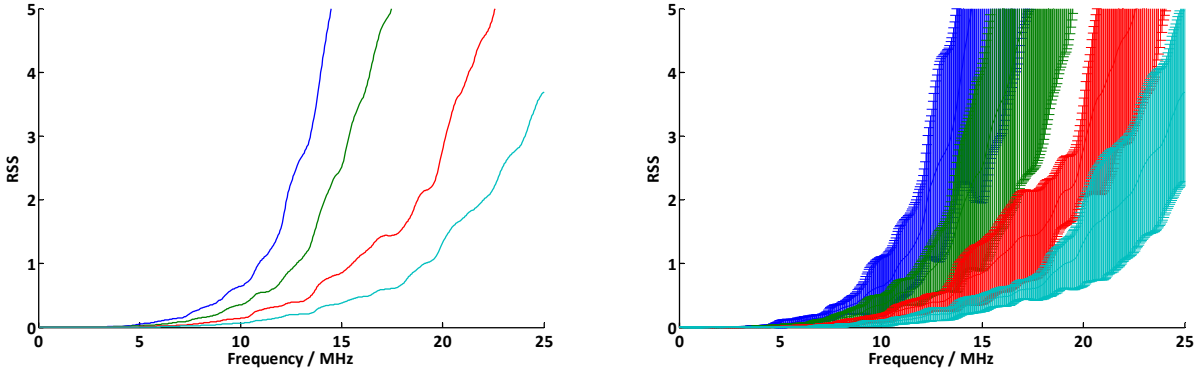

(a) (b)

Figure 5 The mean sum of squared residuals (RSS) as a function of frequency (bandwidth) for 10 μm radius cavities for concentrations of [1,2,5,10 %] shown in [blue, green, red, light blue] respectively; (a) mean of 15 simulations (b) mean+/- one standard deviation.

4. Conclusions

We have shown the results of simulations of the back scattered acoustic response from a slab region containing cavities in a solid matrix. The simulations have shown the emergence of the coherent response for even a single realisation of scatterer locations, under certain conditions. As expected, coherence results where there is small radius, higher concentration and lower frequency (longer wavelength). The degree of incoherence has been quantified and used to determine a maximum frequency at which coherence could be expected for a single realisation of scatterers for specific cavity radius and concentrations. The dependence on radius and concentration was compared with the criterion that the wavelength should be large compared with the average interparticle spacing; the fit showed similar trends but was not quantitatively accurate. We have also shown the significant variability in the degree of incoherence between multiple realisations of the same system (radius, concentration). Different realisations can produce quite different degrees of coherence. Although the model includes some simplifications, it has enabled some interesting features of the response of single realisations of scatterers to be explored.

References

[1] Foldy L L 1945 The multiple scattering of waves *Phys. Rev.* **67** 107-19
[2] Fikioris J G and Waterman P C 1964 Multiple scattering of waves II. "Hole corrections" in the scalar case *J. Math. Phys.* **5** 1413-20
[3] Lloyd P and Berry M V 1967 Wave propagation through an assembly of spheres IV Relations between different multiple scattering theories *Proc. Phys. Soc., London* **91** 678-88
[4] Linton C M and Martin P A 2006 Multiple scattering by multiple spheres: A new proof of the Lloyd- Berry formula for the effective wavenumber *SIAM J. Appl. Math.* **66** 1649-68
[5] Parnell W J and Abrahams I D 2010 Multiple point scattering to determine the effective wavenumber and effective material properties of an inhomogeneous slab *Wave Random Complex* **20** 678-701
[6] Pinfield V J and Challis R E 2011 Acoustic scattering by a spherical obstacle: Modification to

the analytical long-wavelength solution for the zero-order coefficient *J. Acoust. Soc. Am.* **129** 1851-6

[7] Pinfield V J and Challis R E 2012 Simulation of incoherent and coherent backscattered response of cavities in a solid matrix. *J. Acoust. Soc. Am.* **132** 3760-3769

[8] Ying C F and Truell R 1956 Scattering of a plane longitudinal wave by a spherical obstacle in an isotropically elastic solid *J. Appl. Phys.* **27** 1086-97

[9] Challis R E, Povey M J W, Mather M L and Holmes A K 2005 Ultrasound techniques for characterizing colloidal dispersions *Rep. Prog. Phys.* **68** 1541-637